

A NUMERICAL STUDY OF NON-DARCIAN NATURAL CONVECTION IN A VERTICAL ENCLOSURE FILLED WITH A POROUS MEDIUM

C. Beckermann, R. Viskanta, and S. Ramadhyani
Heat Transfer Laboratory, School of Mechanical Engineering,
Purdue University, West Lafayette, Indiana 47907

A numerical study of non-Darcian natural convection in a vertical enclosure filled with a porous medium is performed. The flow is modeled using the Brinkman-Forchheimer-extended Darcy equations. The governing equations are solved with the SIMPLER algorithm and good agreement with previously reported numerical and experimental results is found. An order of magnitude analysis and the numerical results demonstrate the importance of non-Darcian effects. For high Darcy numbers ($Da > 10^{-4}$), both extensions are of the same order of magnitude and must be used simultaneously. In addition, Forchheimer's extension must be included for $Pr \leq 1.0$ and all Darcy numbers. Finally, Nusselt number correlations are presented for three different ranges of the Darcy number covering wide ranges of the governing parameters.

INTRODUCTION

Natural convection in vertical enclosures filled with a porous medium attracts a great deal of research attention because of the fundamental nature of the problem and the broad range of applications, including geothermal systems, fiber and granular insulations, storage of nuclear waste materials, solidification of castings, and electronic cooling. Most of the theoretical work has been based on the assumption of the validity of Darcy's law [1-10]. There are relatively few experimental studies of heat transfer in vertical porous cavities [11-14] and, as noted by Prasad et al. [15], the experimental results for systems other than the glass-water system at low Darcy-Rayleigh numbers have never agreed with the theoretical results obtained with the Darcy model. This has led to the inclusion of inertia and viscous diffusion effects in recent studies of natural convection in porous enclosures [16-22]. Chan et al. [16], Tong and Subramanian [17], and Lauriat and Prasad [18] have studied the viscous effects by using the Brinkman-extended Darcy equations. Tong and Subramanian [17] found that the pure Darcy analysis is applicable only when $RaDa^2/A < O(10^{-4})$. The inertia effects have been investigated by Poulikakos and Bejan [19, 20] through the inclusion of Forchheimer's extension.

Beckermann et al. [22] have shown that at high Darcy numbers the inertia and viscous terms must be included simultaneously to obtain realistic predictions of the

This work was supported in part by the National Science Foundation under grant no. CBT-8313573. Computer facilities were made available by Purdue University Computer Center.

Continuity:
$$\frac{\partial U}{\partial x} + \frac{\partial V}{\partial y} = 0 \tag{1}$$

Momentum:
$$0 = -\frac{\partial P}{\partial y} + \mu_{\text{eff}} \left(\frac{\partial^2 U}{\partial x^2} + \frac{\partial^2 U}{\partial y^2} \right) - \left(\frac{\mu_f}{K} + \frac{\rho C}{\sqrt{K}} |U| \right) U \tag{2}$$

$$0 = -\frac{\partial P}{\partial y} + \mu_{\text{eff}} \left(\frac{\partial^2 V}{\partial x^2} + \frac{\partial^2 V}{\partial y^2} \right) + \rho g \beta (T - T_c) - \left(\frac{\mu_f}{K} + \frac{\rho C}{\sqrt{K}} |U| \right) V \tag{3}$$

Energy:
$$\rho c_{pf} \left(U \frac{\partial T}{\partial x} + V \frac{\partial T}{\partial y} \right) = k_{\text{eff}} \left(\frac{\partial^2 T}{\partial x^2} + \frac{\partial^2 T}{\partial y^2} \right) \tag{4}$$

where
$$|U| = \sqrt{U^2 + V^2} \tag{5}$$

The value of the inertia coefficient C in Forchheimer's extension [see Eqs. (2) and (3)] has been measured experimentally by Ward [23]. Although it is now generally accepted that C is a function of the microstructure of the porous medium [25, 26], Ward found that for a large variety of porous media C can be taken as a constant equal to approximately 0.55. This value is used in all calculations in this paper. While the value of μ_{eff} in Brinkman's extension in the momentum equation remains controversial [26], as a first approximation μ_{eff} is taken equal to μ_f in the present study. With this simplification, the governing equations can be written in dimensionless form as follows:

Continuity:
$$\frac{\partial u}{\partial \xi} + \frac{\partial v}{\partial \eta} = 0 \tag{6}$$

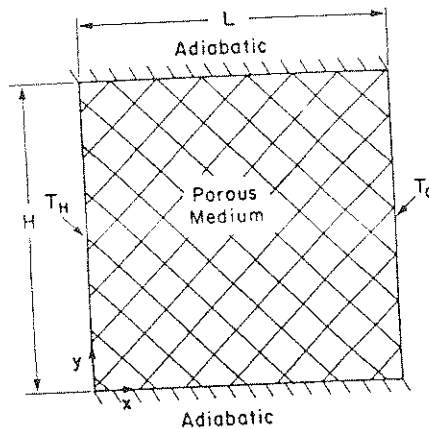


Fig. 1 Schematic of the physical model and coordinate system.

Momentum:

$$0 = -\frac{\partial p}{\partial \xi} + \text{Pr} \left(\frac{\partial^2 u}{\partial \xi^2} + \frac{\partial^2 u}{\partial \eta^2} \right) - \left(\frac{\text{Pr}}{\text{Da}} + \frac{C}{\sqrt{\text{Da}}} |u| \right) u \quad (7)$$

$$0 = -\frac{\partial p}{\partial \eta} + \text{Pr} \left(\frac{\partial^2 v}{\partial \xi^2} + \frac{\partial^2 v}{\partial \eta^2} \right) - \left(\frac{\text{Pr}}{\text{Da}} + \frac{C}{\sqrt{\text{Da}}} |u| \right) v + \text{RaPr}\theta \quad (8)$$

Energy:

$$u \frac{\partial \theta}{\partial \xi} + v \frac{\partial \theta}{\partial \eta} = \frac{\partial^2 \theta}{\partial \xi^2} + \frac{\partial^2 \theta}{\partial \eta^2} \quad (9)$$

The boundary conditions are given in dimensionless form as

$$\begin{aligned} \theta = 1, u = v = 0 & \quad \text{at } \xi = 0, 0 \leq \eta \leq A \\ \theta = 0, u = v = 0 & \quad \text{at } \xi = 1, 0 \leq \eta \leq A \\ \frac{\partial \theta}{\partial \eta} = 0, u = v = 0 & \quad \text{at } \eta = 0, 0 \leq \xi \leq 1 \\ \frac{\partial \theta}{\partial \eta} = 0, u = v = 0 & \quad \text{at } \eta = A, 0 \leq \xi \leq 1 \end{aligned} \quad (10)$$

The results for the total heat transfer rate across the enclosure are presented in terms of the average Nusselt number, defined as

$$\text{Nu} = \frac{hL}{k_{\text{eff}}} = -\frac{1}{A} \int_0^A \frac{\partial \theta}{\partial \xi} \Big|_{\xi=0}^{\xi=1} d\eta \quad (11)$$

From the dimensionless equations (6)–(10) it can be seen that the Nusselt number is a function of four parameters, namely Ra, Da, Pr, and A . In addition, the relative importance of the various terms in the momentum equations (7) and (8) can be examined by an order of magnitude analysis. The magnitude of Forchheimer's extension varies with the square root of Da, while the magnitude of Brinkman's extension is directly proportional to Da (with the Darcy term being of the order of unity). Thus, for Da and $\sqrt{\text{Da}} \ll 1$, Brinkman's and Forchheimer's extensions are insignificant compared to the Darcy term and Darcy's law is applicable. Note that for any Darcy number less than unity, the magnitude of Forchheimer's extension is greater than the magnitude of Brinkman's extension. For very high Darcy numbers, that is, Da and $\sqrt{\text{Da}} = O(1)$, Forchheimer's and Brinkman's extensions are of the same magnitude as the Darcy term. In this high Darcy number regime, both extensions must be used simultaneously and neglecting one extension in favor of the other will lead to serious errors. This order of magnitude analysis also shows that the functional relationship $\text{Nu} = \text{Nu}(\text{Ra}, \text{Da}, \text{Pr}, A)$ will take different forms for the Darcy number regimes established above (see the Results and Discussion section). In addition, as expected, the relative importance of the

inertia term, modeled through Forchheimer's extension, increases with decreasing Prandtl number.

NUMERICAL PROCEDURE

The governing equations (6)-(10) were solved using the SIMPLER algorithm [27]. The mesh size required for sufficient numerical accuracy depended mainly on the Rayleigh and Darcy numbers. A grid of 25×25 to 50×50 nodal points ensured independence of the solution on the grid. The nodal points were uniformly distributed in the y direction, while the distribution along the x direction was slightly skewed to have a greater concentration of points near the vertical boundaries. The iteration procedure was terminated when the dependent variables agreed to four significant digits. Convergence of the numerical solution was also checked by comparing the Nusselt numbers obtained along the two vertical sidewalls; see Eq. (11). The agreement between the two values was always better than 0.1%. The calculations were performed on a CYBER 205 digital computer and required less than 250 CPU seconds.

The accuracy of the numerical algorithm was obtained by comparing the present results for the Nusselt number with values reported in the literature. Table 1a shows a comparison with numerical results based on the pure Darcy formulation (i.e., $\mu_{\text{eff}} = C = 0$). In this case the solution becomes independent of the Prandtl number, and the Rayleigh and Darcy numbers can be collapsed into a single parameter, $Ra_D = RaDa$, often called the Darcy-Rayleigh number. In Table 1a the values for the Nusselt number of Prasad and Kulacki [9] were read from a graph. Considering the large scatter of the data, the agreement with the present results is very good.

In Table 1b previous numerical and experimental results are compared with present predictions for cases where both Darcian and non-Darcian formulations have been used to predict the Nusselt number. The results of Weber [2] and Shiralkar et al. [8] were obtained using the pure Darcy model, while Tong and Subramanian [17] performed a boundary-layer analysis using the Brinkman-extended Darcy model. Klarsfeld's results [12] are actual experimental data. The Prandtl number was estimated from the information reported in [12], while the other dimensionless parameters were given explicitly. In cases 1 and 2 in Table 1b, the present results (obtained with the Brinkman and Forchheimer extensions) show some improvement over the previously reported solutions when compared to the experimental data. In all cases the present values of the Nusselt number are below the experimental data, and in cases 3 and 4 Tong and Subramanian's results agree with the experimental data better than do the present results. As noted by Shiralkar et al. [8], some of the discrepancy between the numerical and experimental values may be due to viscosity variations (about 10%) in the experiments of Klarsfeld. Overall, the present results agree to within 5% with the experimental data. It should be noted that the cases shown in Table 1b are actually fairly close to the Darcy regime, hence the differences between the Nusselt numbers obtained with the various models are expected to be relatively small. There is a lack of experimental data for non-Darcian natural convection in vertical enclosures, which makes a definitive test of the accuracy of the present model difficult.

Table 1 Comparisons of Nusselt Numbers Between Present and Previously Published Results

(a) Pure Darcy formulation, $A = 1.0$									
$Ra_D = RaDa$		Present results (25 × 25 grid)	Walker and Homsey [3]	Shiralkar et al. [8]	Prasad and Kulacki [9]				
50		1.981	1.98	—	≈ 2.0				
100		3.113	3.097	3.115	≈ 3.2				
200		5.038	4.89	4.976	≈ 5.3				
500		9.308	8.66	8.944	≈ 9.3				
2,500		23.64	≈ 24.5	22.660	≈ 24.6				
10,000		48.90	≈ 50.5	—	≈ 50.5				
(b) Other results									
Case	Ra	Da	Pr	A	Weber [2]	Shiralkar et al. [8]	Tong and Subra- manian [17]	Klarsfeld [12]	Present results (26 × 26)
1	1.598×10^9	8.125×10^{-7}	≈ 4	2.25	13.9	10.89	13.5	11.8	11.15
2	1.997×10^9	8.125×10^{-7}	≈ 4	2.25	15.5	12.31	15.0	13.3	12.61
3	9.969×10^7	3.250×10^{-6}	≈ 4	4.5	4.9	—	4.8	4.7	4.54
4	1.994×10^8	3.250×10^{-6}	≈ 4	4.5	6.9	—	6.8	6.8	6.62

RESULTS AND DISCUSSION

Importance of Non-Darcian Effects

Table 2 shows some representative numerical results that demonstrate the effects of the Forchheimer and Brinkman extensions on the Nusselt number. Four different cases are considered: (1) no extensions, (2) Forchheimer's extension only ($C = 0.55$), (3) Brinkman's extension only ($C = 0.00$), and (4) both extensions. The Rayleigh and Darcy numbers were chosen to maintain a constant $RaDa$ product. Thus, with the pure Darcy model (i.e., no extensions) the same Nusselt number is obtained in all cases.

From Table 2 it can be seen that the effect of Brinkman's extension (without inertia effects, i.e., $C = 0.00$) on the Nusselt number is most pronounced at $Da = 10^{-1}$ (90% reduction) and $Da = 10^{-4}$ (49% reduction), while there is basically no effect at $Da = 10^{-8}$. As expected, the Prandtl number has no influence on the Nusselt number if inertia effects are not included ($C = 0.00$). These results are in agreement with Tong and Subramanian [17], who proposed that $RaDa^2/A < O(10^{-4})$ be used as a criterion for the validity of Darcy's law (with inertia effects not considered).

Through the inclusion of Forchheimer's extension, the effects of inertia forces and hence of the Prandtl number on the flow and heat transfer are modeled. In the high Prandtl number limit ($Pr > 1000$), inertia effects are negligible and the Nusselt number approaches the values obtained without Forchheimer's extension (i.e., $C = 0.00$). On the other hand, for $Pr = 1.0$ the influence of Forchheimer's extension (without viscous effects, i.e., $\mu_{eff} = 0.00$) on the Nusselt number is very large at $Da = 10^{-1}$ and 10^{-4} (82 and 57% reductions, respectively) and is relatively small at $Da = 10^{-8}$ (2.2% reduction). For $Pr = 0.01$ the effect of Forchheimer's extension is even more pronounced and the inertia effects must be included at $Da = 10^{-8}$ (26% reduction). In general, inertia effects are important for $Re = |U|\sqrt{Da} C/Pr > 1$ [28, 29].

Table 2 also shows that for large Darcy numbers and $Pr \leq 1.0$ (cases 1 and 2), both extensions must be included simultaneously to obtain realistic results for the Nusselt number. For $Da \leq 10^{-4}$ (cases 3 to 6) the Nusselt numbers obtained with Forchheimer's extension alone are within 3% of the results obtained with both extensions, indicating that the effect of Brinkman's extension is small if Forchheimer's extension is included. This is further illustrated by the fact that in cases 3 and 4 ($Da = 10^{-4}$) the Nusselt numbers obtained with Brinkman's extension alone are significantly higher than the values obtained with both extensions. This discussion shows that Forchheimer's extension should always be included if $Pr \leq 1.0$. For large Prandtl numbers, however, Brinkman's extension alone yields realistic results for the Nusselt number. For large Darcy numbers (and $Pr \leq 1$) both extensions are of the same order of magnitude, while for $Da \leq 10^{-4}$ Forchheimer's extension becomes dominant over Brinkman's extension. Note that these conclusions are in agreement with the order of magnitude analysis presented in the Governing Equations section.

The importance of the non-Darcian effects are further demonstrated by the streamlines and isotherms shown in Figs. 2-4 for cases 5, 3, and 1 of Table 2. For pure Darcian flow, there would be no difference between the three cases considered. With both extensions included, however, the flow patterns change drastically with increasing Darcy number. For $Da = 10^{-8}$ (Fig. 2) the viscous effects are confined to thin boundary layers close to the walls. The isotherms show a thermally stratified core region and sharp temperature gradients along the vertical sidewalls. Obviously, this case is fairly close to

Table 2 Effect of Brinkman's and Forchheimer's Extensions on the Nusselt Number ($A = 1.0$)

Case	Ra	Da	Pr	Without Brinkman's extension		With Brinkman's extension	
				$C = 0.00$	$C = 0.55$	$C = 0.00$	$C = 0.55$
1	10^5	10^{-1}	1.0	48.90	8.782	4.724	4.385
2	10^5	10^{-1}	0.01	48.90	2.184	4.724	1.642
3	10^8	10^{-4}	1.0	48.90	21.21	24.97	20.59
4	10^8	10^{-4}	0.01	48.90	9.276	24.97	9.152
5	10^{12}	10^{-8}	1.0	48.90	47.82	48.90	47.82
6	10^{12}	10^{-8}	0.01	48.90	36.34	48.90	36.34

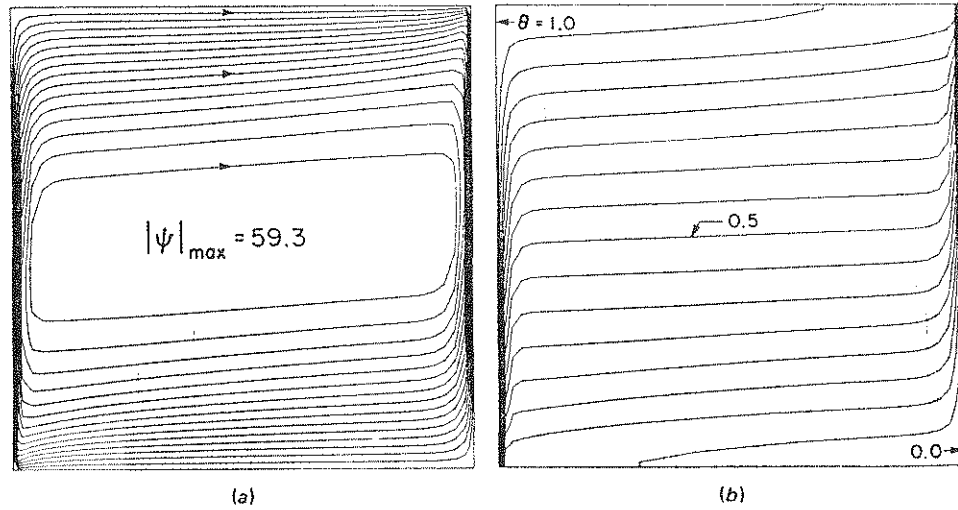


Fig. 2 Numerical results for case 5 of Table 2. (a) Streamlines (equal increments); (b) isotherms (equal increments).

pure Darcian flow and heat transfer. On the other hand, for $Da = 10^{-1}$ (Fig. 4) the viscous forces (modeled through Brinkman's extension) act in the entire cavity and the boundary layers are relatively thick. Accordingly, the core is thermally less stratified and heat transfer due to convection along the horizontal walls has decreased. The flow and heat transfer patterns shown in Fig. 4 are fairly close to what one would expect for natural convection in a vertical enclosure filled with pure fluid at a similar Rayleigh

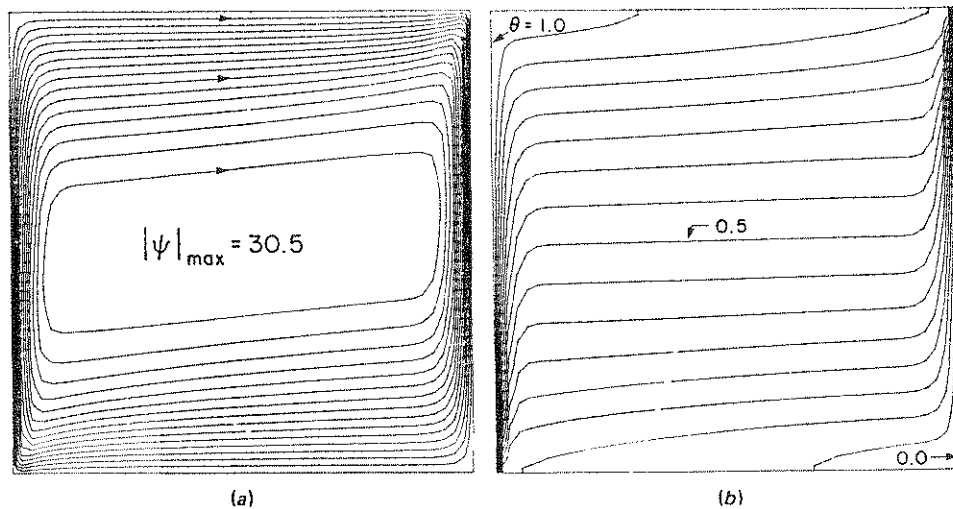


Fig. 3 Numerical results for case 3 of Table 2. (a) Streamlines (equal increments); (b) isotherms (equal increments).

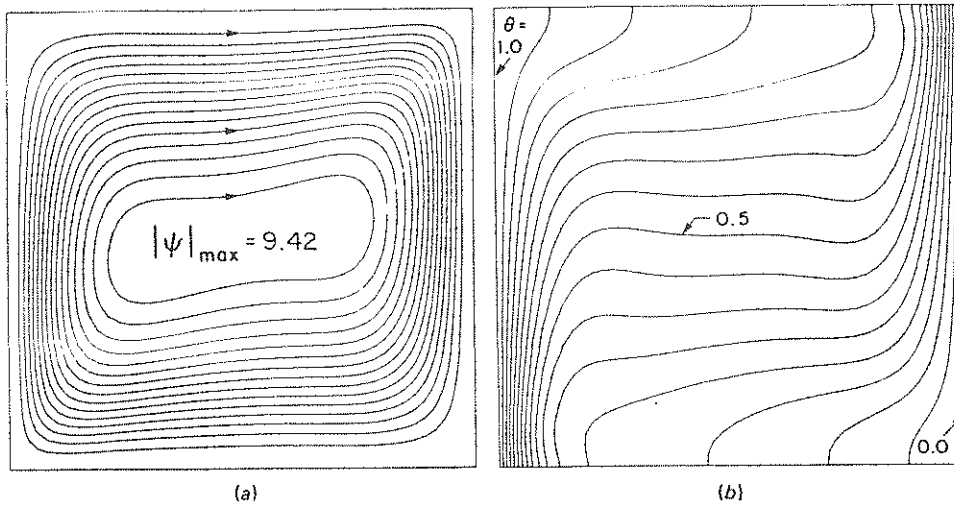


Fig. 4 Numerical results for case 1 of Table 2. (a) Streamlines (equal increments); (b) isotherms (equal increments).

number. This indicates that the Brinkman- and Forchheimer-extended Darcy equations reduce to the correct limit for an infinite permeability (and Darcy number).

Nusselt Number Correlations

A parametric study was performed to investigate the influence of Ra , Da , Pr , and A on the Nusselt number. In Fig. 5 the Nusselt number is plotted against the Darcy and Rayleigh numbers (for $Pr = A = 1.0$). For a fixed product $RaDa$, the Nusselt number increases with increasing Rayleigh number and decreases with increasing Darcy number. For small Darcy numbers, the curves of constant $RaDa$ become horizontal, indicating that in the Darcian regime the Nusselt number is a function of $Ra_D = RaDa$ only. For the Darcian regime, Walker and Homsey [3] correlated their numerical results for $A = 1.0$ according to

$$Nu = 0.51(RaDa)^{1/2} \quad (12)$$

which is in agreement with the above finding. In the non-Darcian regime (i.e., for higher Darcy numbers), however, the slopes of the curves of $\ln Nu$ versus $\ln Da$ or $\ln Ra$ change continuously. Hence Ra and Da become independent parameters with their exponents being a function of Da (or Ra). Nonetheless, an attempt was made to correlate the present results for different ranges of the Darcy number. A total of 143 computational runs were performed covering a broad range of the governing parameters. The Nusselt numbers were correlated according to

$$Nu = aRa^b Da^c A^d \left(\frac{Pr}{e + Pr} \right)^f \quad (13)$$

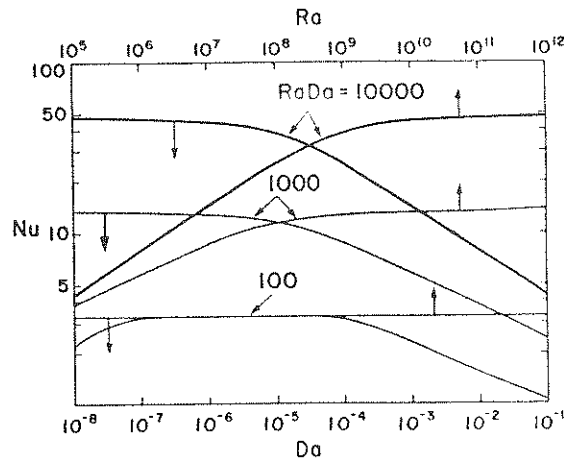


Fig. 5 Effects of the Darcy and Rayleigh numbers on the Nusselt number ($Pr = A = 1.0$).

The values of the coefficients a to f were obtained from a least-squares fit of the numerical results and are listed in Table 3. From an examination of Fig. 5, it was decided to correlate the Nusselt numbers for three ranges of the Darcy number (Table 3). A further subdivision of the data would not have resulted in a significant improvement in the mean deviation of the correlations. The present numerical results are believed to be of about the same accuracy as the correlations presented in Table 3. A plot of the correlations together with the numerical data is shown in Fig. 6. The large discontinuities between the lines for each correlation are due to the different ordinates used for the three correlations. Note that the Nusselt number should always exceed unity. If a certain combination of Ra , Da , A , and Pr results in a Nusselt number below unity, the heat transfer is by pure conduction and the Nusselt number is actually equal to unity. For example, the lower the Darcy number, the larger is the Rayleigh number required for Nu to exceed unity.

An examination of the magnitude of the exponents of the governing parameters (Table 3) reveals several interesting features of the correlations. For example, the exponent of the Rayleigh number changes from 0.315 for large Darcy numbers (correlation 1) to 0.538 for small Darcy numbers (correlation 3). The first value is very close to that reported for vertical enclosures filled with pure fluid, while the latter is close to the theoretical value for the Darcian regime [see Eq. (12)]. A similar observation was made by Prasad et al. [15]. In addition, the influence of the Darcy number increases with decreasing Darcy number. In correlation 1 the exponent of Da is only 0.1, while in correlation 3 the value is very close to the exponent of the Rayleigh number (i.e., 0.53), indicating that in correlation 3 the influence of the extensions is very small and the pure Darcian regime is reached. The importance of Forchheimer's extension can be seen clearly by examining the Prandtl number dependences in the correlations (see also the preceding section, on non-Darcian effects). As in pure fluid enclosures, the Prandtl number has very little influence on the Nusselt number for $Pr > 1$. This has been accommodated by choosing the general form of the correlations as shown in Eq. (13).

Table 3 Coefficients for the Nusselt Number Correlation, Eq. (13)

Correlation	Ranges of the governing parameters						No. of data points	Mean deviation (%)				
	Da	Ra	A	Pr	a	b			c	d	e	f
1	$10^{-1} \geq Da \geq 10^{-3}$	$10^3 \leq Ra \leq 10^8$	$1 \leq A \leq 10$	$0.01 \leq Pr \leq 10,000$	0.170	0.315	0.10	-0.36	0.45	0.32	46	8.59
2	$10^{-4} \geq Da \geq 10^{-6}$	$10^6 \leq Ra \leq 10^{10}$	$1 \leq A \leq 10$	$0.01 \leq Pr \leq 10,000$	0.191	0.425	0.33	-0.36	0.45	0.23	37	9.35
3	$10^{-7} \geq Da \geq 10^{-10}$	$10^9 \leq Ra \leq 10^{14}$	$1 \leq A \leq 10$	$0.01 \leq Pr \leq 10,000$	0.281	0.538	0.53	-0.36	0.45	0.06	60	7.90

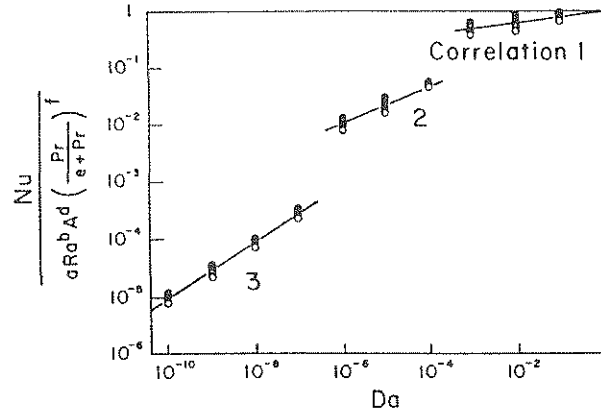


Fig. 6 Comparison of predicted Nusselt numbers with correlations.

For $Pr \leq 1$ and large Darcy numbers (correlation 1), however, the Prandtl number dependence is very strong. The influence of Pr becomes less for decreasing Darcy numbers. For $Da < 10^{-7}$ (correlation 3) the Prandtl number dependence is very weak, indicating again that the pure Darcian regime is reached. In general, the exponents of Ra , Da , and $Pr/(0.45 + Pr)$ are expected to vary continuously from their values at very high Darcy numbers (e.g., $Da = 10^{-1}$) to the values for pure Darcian flows (see also Fig. 5). Hence, a more accurate correlation covering the entire range of Darcy numbers might be obtained by including the dependence of the exponents on the Darcy number in Eq. (13). Because of the complicated nature of these exponents, a reasonable fit of the Nusselt number data for a correlation of this form has not been found.

CONCLUSIONS

A numerical study of non-Darcian natural convection in a vertical porous enclosure is performed. The Brinkman-Forchheimer-extended Darcy equations are solved using the SIMPLER algorithm and good agreement with previously reported numerical and experimental results is found. An order of magnitude analysis and the numerical results clearly show the importance of the non-Darcian effects for high Darcy numbers ($Da > 10^{-7}$). Through the inclusion of Forchheimer's extension, the effect of the Prandtl number on the heat transfer is investigated for the first time and is found to be important at $Pr \leq 1$. In addition, it is shown that for large Darcy numbers ($Da > 10^{-4}$), both extensions must be used simultaneously to obtain realistic heat transfer results.

In a parametric study, the dependence of the Nusselt number on the governing parameters Ra , Da , A , and Pr is investigated. It is found that the influence of Ra , Da , A , and Pr on Nu changes continuously with decreasing Darcy number up to the point where the pure Darcian regime is reached (i.e., $Da \leq 10^{-8}$). A set of three correlations for calculating the Nusselt number is proposed for three ranges of the Darcy number. These correlations should provide reasonable estimates of the Nusselt number for most practical purposes.

REFERENCES

1. G. C. Bankvall, Natural Convection in Vertical Permeable Space, *Waerme Stoffuebertrag.*, vol. 7, pp. 22-30, 1974.
2. J. E. Weber, The Boundary-Layer Regime for Convection in a Vertical Porous Layer, *Int. J. Heat Mass Transfer*, vol. 18, pp. 569-573, 1975.
3. K. L. Walker and G. M. Homsey, Convection in a Porous Cavity, *J. Fluid Mech.*, vol. 87, pp. 449-474, 1978.
4. A. Bejan, On the Boundary Layer Regime in a Vertical Enclosure Filled with a Porous Medium, *Lett. Heat Mass Transfer*, vol. 6, pp. 93-102, 1979.
5. P. G. Simpkins and P. A. Blythe, Convection in a Porous Layer, *Int. J. Heat Mass Transfer*, vol. 23, pp. 881-887, 1980.
6. C. E. Hickox and D. K. Gartling, A Numerical Study of Natural Convection in a Horizontal Porous Layer Subjected to an End-to-End Temperature Difference, *ASME J. Heat Transfer*, vol. 103, pp. 797-802, 1981.
7. P. A. Blythe, P. G. Simpkins, and P. G. Daniels, Thermal Convection in a Cavity Filled with a Porous Medium: A Classification of Limiting Behaviors, *Int. J. Heat Mass Transfer*, vol. 26, pp. 701-708, 1983.
8. G. S. Shiralkar, M. Haajizadeh, and C. L. Tien, Numerical Study of High Rayleigh Number Convection in a Vertical Porous Enclosure, *Numer. Heat Transfer*, vol. 6, pp. 223-234, 1983.
9. V. Prasad and F. Kulacki, Natural Convection in a Vertical Porous Annulus, *Int. J. Heat Mass Transfer*, vol. 27, pp. 207-219, 1984.
G. Rajen, Natural Convection in Porous Media Using the Boundary Element Method, AIAA New York, Paper No. AIAA-86-1263, 1986.
11. K. J. Schneider, Investigation of the Influence of Free Thermal Convection on Heat Transfer Through Granular Material, *Proc. Int. Inst. Refrig.*, pp. 247-253, 1963.
12. S. Klarsfeld, Champs de Temperature Associes aux Mouvements de Convection Naturelle Dans In Milieu Poreux Limite, *Rev. Gen. Therm.*, vol. 9, pp. 1403-1423, 1970.
13. S. A. Bories and M. A. Combarous, Natural Convection in a Sloping Porous Layer, *J. Fluid Mech.*, vol. 57, pp. 63-79, 1973.
14. N. Seki, S. Fukusako, and H. Inaba, Heat Transfer in a Confined Rectangular Cavity Packed with Porous Media, *Int. J. Heat Mass Transfer*, vol. 21, pp. 985-989, 1978.
15. V. Prasad, F. Kulacki, and M. Keyhani, Natural Convection in Porous Media, *J. Fluid Mech.*, vol. 150, pp. 89-119, 1985.
16. B. K. C. Chan, C. M. Ivey, and J. M. Barry, Natural Convection in Enclosed Porous Media with Rectangular Boundaries, *ASME J. Heat Transfer*, vol. 92, pp. 21-27, 1970.
17. T. W. Tong and E. Subramanian, A Boundary-Layer Analysis for Natural Convection in Vertical Porous Enclosures—Use of the Brinkman-Extended Darcy Model, *Int. J. Heat Mass Transfer*, vol. 28, pp. 563-571, 1985.
18. G. Lauriat and V. Prasad, Natural Convection in a Vertical Porous Cavity: A Numerical Study for Brinkman-Extended Darcy Formulation, in V. Prasad and N. A. Hussain (eds.), *Natural Convection in Porous Media*, pp. 13-22. ASME, New York, 1986.
19. D. Poulikakos, A Departure from the Darcy Model in Boundary Layer Natural Convection in a Vertical Porous Layer with Uniform Heat Flux from the Side, *ASME J. Heat Transfer*, vol. 107, pp. 716-720, 1985.
20. D. Poulikakos and A. Bejan, The Departure from Darcy Flow in Natural Convection in a Vertical Porous Layer, *Phys. Fluids*, in press.
21. J. Georgiadis and I. Catton, Prandtl Number Effect on Benard Convection in Porous Media, *ASME J. Heat Transfer*, vol. 108, pp. 284-290, 1986.

22. C. Beckermann, S. Ramadhyani, and R. Viskanta, Natural Convection Flow and Heat Transfer Between a Fluid Layer and a Porous Layer Inside a Rectangular Enclosure, in V. Prasad and N. A. Hussain (eds.), *Natural Convection in Porous Media*, pp. 1-12, ASME, New York, 1986.
23. J. C. Ward, Turbulent Flow in Porous Media, *J. Hydraul. Div. ASCE*, vol. 90, pp. 1-12, 1964.
24. G. S. Beavers and E. M. Sparrow, Non-Darcy Flow through Fibrous Porous Media, *J. Appl. Mech.*, vol. 36, pp. 711-714, 1969.
25. S. Ergun, Fluid Flow Through Packed Columns, *Chem. Eng. Prog.*, vol. 48, pp. 89-94, 1952.
26. S. Kim and W. B. Russell, Modelling of Porous Media by Renormalization of the Stokes Equations, *J. Fluid Mech.*, vol. 154, pp. 269-286, 1985.
27. S. Patankar, *Numerical Heat Transfer and Fluid Flow*, Hemisphere, Washington, D.C., 1980.
28. P. Cheng, Heat Transfer in Geothermal Systems, *Adv. Heat Transfer*, vol. 14, pp. 1-105, 1978.
29. C. Beckermann and R. Viskanta, Forced Convection Boundary Layer Flow and Heat Transfer Along a Flat Plate Embedded in a Porous Medium, submitted for publication in *Int. J. Heat Mass Transfer*.

Received June 21, 1986
Accepted August 11, 1986